Improved comparison of P and *P* charge-to-mass ratios

Physica Scripta. Vol. T59, 307–310, 1995

Improved Comparison of $\bar{P}$ and P Charge-to-Mass Ratios

D. Phillips, W. Quint* and G. Gabrielse

Department of Physics, Harvard University, Cambridge, MA 02138

H. Kalinowsky and G. Rouleau†

Institut für Physik, Universität Mainz, 55099 Mainz, Germany

and

W. Jhe

Department of Physics, Seoul National University, Seoul 151-742, Korea

Received December 16, 1994; accepted February 20, 1995

Abstract

The measured ratio of charge-to-mass ratios for the antiproton and proton is 1.000 000 001 5 ± 0.000 000 001 1. This 1 part in 10^9 comparison (1 ppb) is possible because a single $\bar{p}$ or p is now directly observed while trapped in an open access Penning trap. The comparison is the most accurate mass spectrometry of particles with opposite charge and is the most sensitive test of CPT invariance for a baryon system. It is 40 times more accurate than our earlier comparison with many trapped antiprotons and protons, and is more than 45 000 times more accurate than earlier comparisons made with other techniques.

1. Introduction

A new and greatly improved comparison of the charge-to-mass ratios of the antiproton ($\bar{p}$) and proton (p) has been completed [1]. The first such comparison took place at the discovery of the antiproton [2], which was identified by comparing its charge-to-mass ratio (q/M) to that of the proton (p). The accuracy of the mass comparison (Fig. 1) increased when transition energies were measured for antiprotons orbiting as "heavy electrons" in exotic atoms [3–6]. The charge-to-mass ratios for $\bar{p}$ and p were compared more than 1000 times more accurately when our TRAP collaboration developed the slowing, trapping, cooling and stacking techniques [7–9] to reduce by 10^{10} the energy of 5.9 MeV antiprotons from the unique LEAR facility of CERN, yielding more than 10^5 trapped $\bar{p}$ at 4.2 K. The cyclotron frequencies $\nu_c = qB/(2\pi M)$ of approximately 100 trapped antiprotons and protons were compared to 4×10^{-8} in the same magnetic field B [10].

Comparing a measured ν_c for a single trapped $\bar{p}$ and p now makes it possible to compare their charge-to-mass ratios 40 times more accurately, an improvement by a factor of 45 000 over the exotic atoms measurements. Special relativity is crucial in that ν_c depends upon the "relativistic mass" $M = \gamma M_0$, where $\gamma = 1/\sqrt{1 - v^2/c^2}$ is the familiar function of the particle's speed v normalized to that of light c [11, 12]. Detected cyclotron excitations of 1 eV to 200 eV are such low kinetic energies as to be generally regarded as exceedingly nonrelativistic, with $\gamma < 1.000\,000\,2$. However, the cyclotron frequency of one trapped $\bar{p}$ or p is measured with a resolution so high ($< 2 \times 10^{-10}$) that the relativistic frequency shift is inescapably large, providing an especially clean demonstration of special relativity along with the greatly improved comparison of $\bar{p}$ and p.

By four orders of magnitude, the new measurement is the most precise test of CPT invariance made with baryons, with C, P and T representing charge conjugation, parity and time reversal transformations. The invariance of physical laws under CPT transformations is widely assumed to be true, despite the possibility to violate P, CP and T separately, because it is not possible to construct a Lorentz invariant, local field theory which is not invariant under CPT

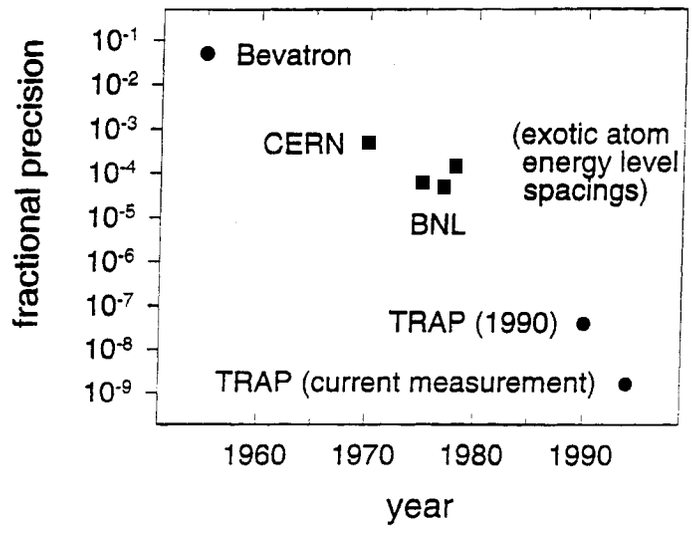

Fig. 1. Comparisons of charge-to-mass ratios (circles) and inertial masses (squares) for $\bar{p}$ and p.

* Current address: GSI, Planckstrasse 1, D-64291 Darmstadt, Germany.
† Current address: Manne Siegbahn Laboratory, Frescativägen 24, S-10405 Stockholm, Sweden.

[13]. Such invariance implies that the inertial masses and charge magnitudes of a particle and antiparticle are identical, along with their mean lives and magnetic moment magnitudes. Despite the fundamental importance of CPT invariance, precise experimental tests are very scarce [14]. Only one lepton magnetic moment comparison (of e^+ and e^- [15]) and one meson mass comparison (of K_0 and $\bar{K}_0$ [16]) are of comparable or higher fractional precision than the baryon comparison reported here.

Antiprotons, obtained at 5.9 MeV from the low energy antiproton storage ring (LEAR) have their energy reduced to 0.3 milli-eV within our apparatus. They slow below 3 keV in a degrader and are caught in a Penning trap [7], then cool via collisions with cold electrons in the trap [8] to thermal equilibrium at 4.2 K. Typically 10^4 antiprotons reside with approximately 10^7 electrons in the Penning trap. To selectively eject the electrons, which would otherwise disrupt the precision comparison of $\bar{p}$ and p, the voltage on one end of the trap is pulsed to open the trap for 200 ns. The antiprotons remain while the less massive electrons escape.

The open access Penning trap [17] provides a good environment for a precision mass spectrometry along with the access needed to initially admit antiprotons before cooling. It consists of a 5.85 T magnetic field (from a persistent superconducting solenoid) and a superimposed electrostatic quadrupole potential. Trapped particles have three oscillatory motions [12]. The axial motion, at frequency $\nu_z = 954$ kHz, is along the direction of the magnetic field. The trap-modified cyclotron motion, at a higher frequency $\nu_c' = 89.3$ MHz, is a circular motion in a perpendicular plane, as is the magnetron motion at a much lower frequency $\nu_m = 5.1$ kHz. Unlike traditional traps used for precision mass measurements (with electrodes shaped along the hyperbolic equipotentials of the desired quadrupole potential), this trap is made of stacked cylinders, each with the same inner diameter [Fig. 2(a)]. A careful choice of electrode lengths [17] and careful tuning of the applied voltages produces the high quality electrostatic quadrupole needed to produce harmonic motions, with frequencies independent of excitation energy. The observed signal-to-noise in this and related cylindrical configurations are as good as that observed in the hyperbolic traps. A key feature is an orthogonality which keeps the well depth from changing during the tuning. The trap is within a sealed vacuum enclosure kept at 4.2 K by thermal contact to liquid helium, to produce a vacuum that our earlier $\bar{p}$ measurements indicate is better than 5×10^{-17} Torr [10]. (This vacuum allowed storing two antiprotons for 60 days.)

The cyclotron and axial motions of a trapped $\bar{p}$ or p are observed when the induce detectable oscillatory voltages across attached LCR circuits [Fig. 2(a)]. Energy dissipation in the two circuits damps these motions into thermal equilibrium with the tuned circuits near 4.2 K. To maximize the signal and damping, the quality factor (Q) for each circuit is made as large as possible. A circuit resonant at 89.3 MHz with $Q = 800$ is connected to one of four ring sections to detect the cyclotron oscillation. The axial motion is detected similarly except that a nearly resonant driving potential is applied to the endcap opposite the axial detection circuit. To detect the axial motion of one $\bar{p}$ or p, a superconducting inductor and shield have been developed. These are made of the type II superconductor NbTi to allow them to be located near the trap in the 5.85 T field. (To avoid quenching an earlier circuit of type I superconductor, it had to be located in a low field region away from the trap [18]). The minimal capacitance leads to a high $Q = 3000$ at 954 kHz (Fig. 3), and a 1/e damping time for the $\bar{p}$ (or p) of 3 seconds, a four-fold improvement over the copper circuits of the same frequency and physical size.

To reduce the number of trapped antiprotons to one, the cyclotron motion of the antiprotons is excited by a strong, nearly resonant drive pulsed onto a segment of the ring or a compensation electrode. The broad cyclotron response signal is monitored as the trapping well depth is reduced from 18 eV to below 0.3 eV to spill antiprotons. This signal breaks into separate resonance peaks when less than 15 antiprotons remain, each peak due to an excited antiproton with a distinct cyclotron energy and thus a distinct cyclotron frequency because of special relativity. The trapping potential is lowered until only one antiproton is still observed, then restored to 18 V. The trapped particle is radially centered by a strong sideband cooling drive at frequency $\nu_z + \nu_m$ [19] applied to one half of a split compensation electrode.

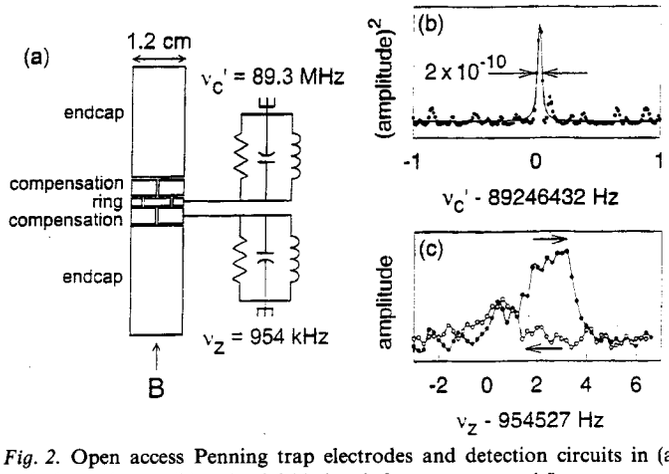

Fig. 2. Open access Penning trap electrodes and detection circuits in (a), with the cyclotron (b) and axial (c) signals from one trapped $\bar{p}$.

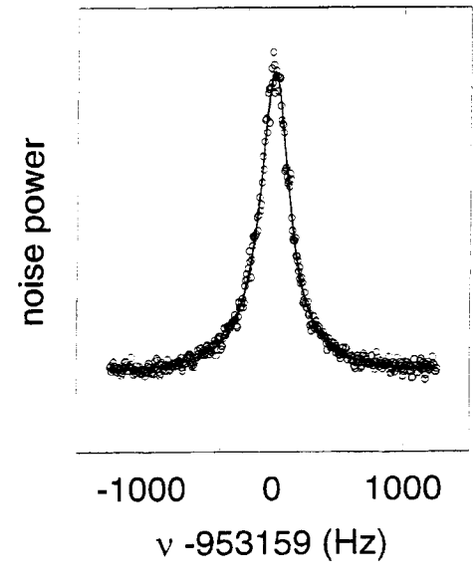

Fig. 3. Johnson noise of the superconducting tuned circuit used to detect and damp the axial motion of $\bar{p}$ and p. The circuit has a high quality factor $Q = 3400$.

One proton is loaded with the trapping potential on the ring switched to -18 V. A keV electron beam from a field emission point (inside the trap's vacuum enclosure) is sent through the trap to strike a surface. Some atoms liberated from this surface collide with the electron beam within the trap volume, are ionized and become trapped. Strong axial noise at frequencies below 850 kHz is applied to one endcap to drive out positive ions which would otherwise load into the trap. (Even one remaining ion prevents an accurate measurement.) Notch and low pass filters reduce this noise by 120 dB at $\nu_z = 954$ kHz to prevent driving out a proton. We alternatively drive and detect at the cyclotron frequency ν_c', switching off the electron beam when a cyclotron signal indicates that one proton is trapped.

The large, undriven cyclotron signal of one trapped $\bar{p}$ [Fig. 2(b)] has a frequency resolution narrower than 2×10^{-10}, limited by the Fourier transform width of the detector. (The measured decay time discussed below corresponds to a much narrower width.) Figure 2c shows driven axial signals for one $\bar{p}$ which differ when the driving force is swept upward and downward in frequency because the trap is not quite tuned to produce a perfect electrostatic quadrupole.

An initially excited cyclotron motion damps exponentially by slowly dissipating energy in the detection circuit. Special relativity shifts ν_c' upward in proportion to the remaining excitation energy E_c, as illustrated by three cyclotron resonances at different times [Fig. 4(a)]. The time dependent ν_c' [Fig 4(b)] is fit to the expected exponential to extract the ν_c' endpoint, the limiting value for vanishing E_c, and the residuals [Fig. 4(c)] are small. Quadratic gradients in the magnetic field (i.e. a "magnetic bottle") and electrostatic anharmonicity similarly couple ν_c' and E_c, but much less strongly.

The compared cyclotron frequency $\nu_c = qB/(2\pi M)$ differs slightly from ν_c' (the cyclotron frequency in the trap), but is related to the three measured frequencies ν_c', ν_z and ν_m by the invariance theorem [20].

$$(\nu_c)^2 = (\nu_c')^2 + (\nu_z)^2 + (\nu_m)^2 \qquad (1)$$

which is independent of the leading perturbations of an imperfect Penning trap (e.g. tilts of the magnetic field and quadratic changes in the trapping potential). Both ν_c' (from a decay endpoint) and the axial frequency ν_z are always measured. Attaining a 1 ppb accuracy in ν_c requires a careful measurement of ν_z to better than 8 Hz, but ν_m needs only be measured to 10% and is thus measured less often.

The 5.85 T magnetic field fluctuates in time because the ambient magnetic field (in which the solenoid is located) is fluctuating. While high frequency fluctuations are shielded by eddy currents induced in various cylindrical conductors surrounding the trap, low frequency fluctuations are potentially very serious. Magnets from the nearby CERN proton synchrotron (PS) are the largest problem, making $4\,\mu T$ (40 mG) fluctuations at our location as often as every 2.4 seconds. The solution is to cancel such fluctuations at the location of the trapped particles by the addition of a superconducting solenoid inductively coupled to the high field solenoid [21]. Currents induced in the coupled superconducting solenoids cancel the effect of spatially uniform fluctuations by a factor of 156 [22], without compromising the homogeneity of the magnetic field. Gradients in the fluctuating fields from nearby sources reduce the shielding of the PS fluctuations to a factor of 110 and the LEAR magnets only several meters away are shielded by a factor of 50. Fluxgate magnetometers monitor the ambient field during a measurement to alert us to external magnetic fluctuations too large to be cancelled by the self-shielding solenoid system.

Magnetic field stability remains a problem even when ambient fluctuations are eliminated. Using a $\bar{p}$ or p as a magnetometer many days shows that the magnetic field varies slowly depending upon the pressure and boil-off rate for the helium reservoirs which cool the superconducting solenoid and keep the trap at 4.2 K. The pressures are thus monitored and regulated over these reservoirs and the solenoid's nitrogen reservoir, and gas flows from the dewars are monitored. Nonetheless, a daily drift in the magnetic field [visible in Fig. 5(a)] correlates with unfortunately large changes in the temperature of the accelerator hall. Such field drifts are slow enough (<2 ppb/hr) to fit to a quadratic or cubic function of time, provided that the temperature regulation for the pressure reference volume does not go out of range. (Two complete p-$\bar{p}$-p comparisons were lost in this way.)

One of the four p-$\bar{p}$-p comparisons which comprise this measurement is shown in Fig. 5(a). The four points to the left are the measured cyclotron frequencies ν_c (each from a fitted ν_c' endpoint and a measured ν_z) for four cyclotron excitations of the same trapped p. A single $\bar{p}$ was then loaded in place of the p, and ν_c' was measured for three cyclotron decays (triangles). A p was again loaded and ν_c measured for

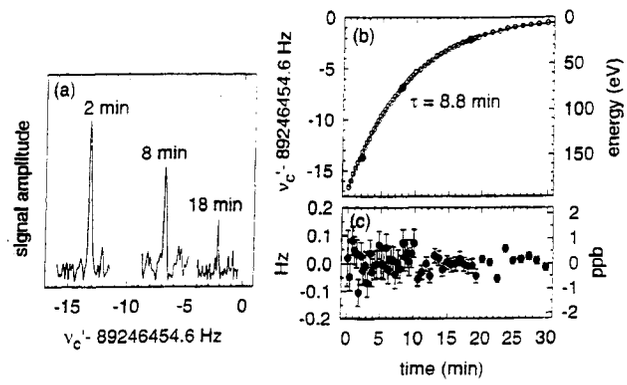

Fig. 4. Special relativity shifts the cyclotron frequency of a single trapped $\bar{p}$ as its cyclotron energy is slowly and exponenally dissipated in the detector. Cyclotron signals for three subsequent times in (a) have frequencies highlighted in the measured frequency *vs.* time points in (b). A fit to the expected exponential has small residuals (c) and gives ν_c' for the limit of no cyclotron excitation.

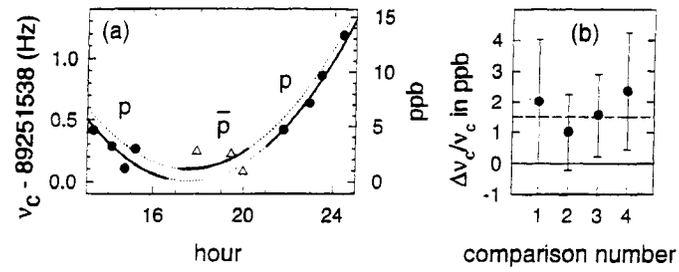

Fig. 5. (a) Measured ν_c for one p, one $\bar{p}$ and then a second p. (b) Fractional differences in ν_c for $\bar{p}$ and p, from four p-$\bar{p}$-p comparisons like that in (a), before correcting for differing locations of $\bar{p}$ and p.

several more cyclotron decays. All ν_c values were then fitted to cubic functions of time as mentioned, with a possible difference $\Delta\nu_c = \nu_c(\bar{p}) - \nu_c(p)$ included as a fitting parameter. Fig. 5(b) shows this difference (n ppb) for the four p-$\bar{p}$-p comparisons. The weighted average and the standard deviation of the points, divided by $\sqrt{4}$, are given by $\Delta\nu_c = 1.5 \pm 0.3$ ppb. (The average decreases by 0.3 ppb if quadratic fits are used instead.)

The largest measurement uncertainty arises because the $\bar{p}$ and p have opposite sign, and thus require externally applied trapping potentials of opposite sign. Reversing the applied potential does not completely reverse the potential experienced by the particle (e.g. due to the patch effect and charges on the inner surfaces of the trap electrodes). During a mass measurement the $\bar{p}$ and p thus reside at slightly different locations, as if an unchanging offset potential was applied to trap electrodes to either side of the particle. If the nearly homogeneous magnetic field differs slightly between the two locations, ν_c for $\bar{p}$ and p will differ even if the charge-to-mass ratios do not.

Both $\bar{p}$ and p are near extrema in the magnetic field. These are useful reference locations since they do not move when the potential reverses. We move $\bar{p}$ and p away from their measurement locations in three orthogonal directions (by applying offset voltages across the endcaps, and across opposite ring quadrants). The measured ν_c as a function of position for each particle reveals its location with respect to the extremum and provides the magnetic field gradients. Figure 6 shows the measured gradients in three orthogonal directions. The measured cyclotron frequency ν_c is plotted as a function of the offset potential applied to move the particle. One radial direction unfortunately still has a "large", nearly linear gradient of 20 ppb/mm (ten times larger than the gradients in orthogonal directions). We estimate that the radial separation between the equilibrium measurement locations for the $\bar{p}$ and p is 50 μm or less. This corresponds to an uncertainty of 1 ppb and to an effective offset potential of 0.2 Volt applied across opposing segments of the ring electrode.

Prior to the p-$\bar{p}$-p comparisons, the current in 9 superconducting shim coils was adjusted in several iterations, to minimize the magnetic gradients in the three orthogonal directions. With more iterations, the largest remaining gradient could be reduced but this long and tedious process takes weeks. The shims are not completely orthogonal and the trap must be retuned at every particle location to make the axial oscillation harmonic enough to measure ν_z. The gradients and relative particle locations did not change noticeably while the trap remained at 4.2 K as long as no cooling electrons hit the trap electrodes.

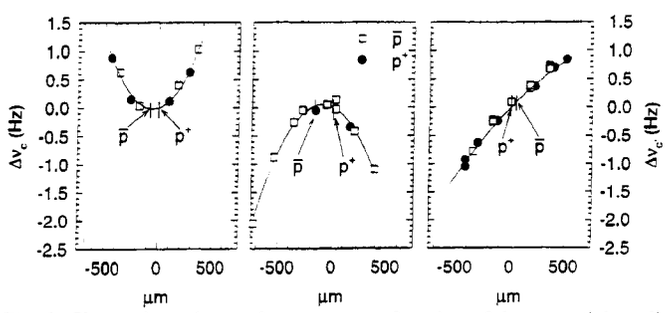

Fig. 6. Change in cyclotron frequency as a function of the potential applied to move a $\bar{p}$ (filled circles and dashed lines) and p (hollow squares and solid lines) away from the center of the trap. The center of oscillation is moved in the axial direction (a), the radial direction with the largest gradient (b), and an orthogonal radial direction (c).

The ratio of the antiproton and proton charge-to-mass ratios (expressed as the mass ratio which is traditional for mass spectrometry) is thus given by

$$M(\bar{p})/M(p) = 0.999\,999\,998\,5\ (11), \qquad (2)$$

with the uncertainty in the last digits in parentheses. As discussed earlier, this ratio represents the most accurate mass spectrometry of particles of opposite sign and is the most accurate test and confirmation of CPT invariance with a baryon system.

For the future, we will compare ν_c for an H^- ion and a $\bar{p}$ stored together in the same trap. The dual advantages of comparing species with the same charge sign, and more rapid switching between species, should allow a precision similar to the 0.1 ppb which has been attained with positive ions loaded for comparison every few minutes [23]. It should thus be possible to deduce a even more accurate comparison of $\bar{p}$ and p despite the special challenges which pertain for mass spectrometry on an exotic species at an accelerator facility.

We are grateful to A. Khabbaz, J. Gröbner and H. Noh for experimental assistance, to L. Lapidus and D. Enzer for help with pressure regulation, and to the CERN laboratory and the LEAR staff for providing 5.9 MeV antiprotons. Support came from the AFOSR, the atomic physics program of the NSF, the German BMFT and KOSEF of Korea.

References

1. Gabrielse, G. *et al.*, (Phys. Rev. Lett. in press)
2. Chamberlain, O., Segre, E., Wiegand, C. and Ypsilantis, T., Phys. Rev. **100**, 947 (1955).
3. Bamberger, A. *et al.*, Phys. Lett. **33B**, 233 (1970).
4. Hu, E. *et al.*, Nucl. Phys. **A254**, 403 (1975).
5. Roberson, P. *et al.*, Phys. Rev. **C16**, 1945 (1977).
6. Roberts, B. L., Phys. Rev. **D17**, 358 (1978).
7. Gabrielse, G. *et al.*, Phys. Rev. Lett. **57**, 2504 (1986).
8. Gabrielse, G. *et al.*, Phys. Rev. Lett. **63**, 1360 (1989).
9. Gabrielse, G. *et al.*, Phys. Rev. **A40**, 481 (1989).
10. Gabrielse, G. *et al.*, Phys. Rev. Lett. **65**, 1317 (1990).
11. Rabi, I. I., Z. Phys. **49**, 507 (1928).
12. Brown, L. S. and Gabrielse, G., Rev. Mod. Phys. **58**, 233 (1986).
13. See e.g. J. Wess, Hyper. Int **44**, 3 (1988).
14. Particle Data Group, Phys. Rev. **D50**, 1228 (1994).
15. Van Dyck Jr., R. S., Schwinberg, P. B. and Dehmelt, H. G., Phys. Rev. Lett. **59**, 26 (1987).
16. Carosi, R. *et al.*, Phys. Lett. **B237**, 303 (1990).
17. Gabrielse, G., Haarsma, L. and Rolston, S. L., Intl. J. of Mass Spec. and Ion Proc., **88**, 319 (1989); *ibid.*, **93**, 121 (1989).
18. Jefferts, S. R., Heavner, T., Hayes, P. and Dunn, G. H., Rev. Sci. Instrum. **64**, 737 (1993).
19. Wineland, D. J. and Dehmelt, H. G., Intl. J. of Mass Spec. and Ion Phys. **16**, 338 (1985); *ibid.*, **19**, 251E.
20. Brown, L. S and Gabrielse, G., Phys. Rev. **A25**, 2423 (1982).
21. Gabrielse, G. and Tan, J., J. of Appl. Phys. **63**, 5143 (1988).
22. Gabrielse, G. *et al.*, J. of Mag. Res. **91**, 564 (1991).
23. DiFilippo, F., Natarajan, V., Boyce, K. R. and Pritchard, D. E., Phys. Rev. Lett. **73**, 1481 (1994).